International Journal of Research in Advanced Engineering and Technology
Online ISSN: 2455-0876
www.engineeringresearchjournal.com
Volume 2; Issue 1; January 2016; Page No. 07-09

Corrosion of Fe-25cr-20ni-0.40c Alloy: An experimental and computational study

[1] C Lanz, [2] G Brizuela1, [*3] S Simonetti

[1, 2, 3] Universidad Nacional del Sur-CONICET, Av. Alem 1253, 8000 Bahía Blanca, Argentina.

[3] Universidad Tecnológica Nacional, Facultad Regional Bahía Blanca, 11 de Abril 461, 8000 Bahía Blanca, Argentina

Abstract
The investigation combines microstructural characterization analyses and atomistic modeling to elucidate the mechanism of carburization embrittlement of an iron-nickel-chromium alloy exposed to high temperature. It was studied an austenitic Fe-25Cr-20Ni-0.40C stainless steel obtained of the tubes of the industrial cracking furnace after 25,000 h of service at 900-1200 ºC. The service-exposed material presented bigger carbides in the austenitic matrix comparing with the as-cast material, cavities between the grains and micro fissures in grain edges, indicating that the material present damage by creep. The theoretical calculations help us to interpret the changes in the alloy electronic structure and the chemical bonding. The atomic orbital occupations of the metallic bonds are affected during carburization. The strengths of the, Cr-Ni, Fe-Cr, Fe-Ni and Ni-Ni bonds nearest neighbors to the carbon atoms are the most affected. The metallic bond weakening is mainly a consequence of the new C-Ni, C-Fe and C-Cr interactions formed after carburization phenomena.

Keywords: microanalysis techniques, computational techniques, iron-nickel-chromium alloy, carburization

1. Introduction

Reformer tubes are generally made from cast creep resistant austenitic steel. Although the furnace tubes are usually designed for a normal life of 100,000 h (11.4 years), their actual service life, however, varies from 30,000 to 180,000 h, depending on the service conditions. Due to prolonged exposure to high temperature, the microstructure of the material is subjected to degradation. In this paper we studied an austenitic Fe-25Cr-20Ni-0.40C stainless steel obtained of the tubes of an industrial cracking furnace, after 25,000 h of service at 900-1200 ºC. We analyzed the changes in the sample microstructure due carburization process using optical and scanning electron microscopy. A complementary theoretical study was also performed. The changes in the alloy electronic structure after service are addressed. The chemical bonding analysis is also considered in order to explain some failures observed experimentally.

2. Experimental Study

The changes in the Fe-25Cr-20Ni-0.40C stainless steel structure were analyzed comparing the as-cast material with the ex-service material (25,000 h of service at 900-1200 ºC). The specimens were analyzed by scanning electron microscopy (SEM) [1, 5] using a microscope JEOL JSM-35CF which operates at voltages between 1,000 V - 50,000 V, currents up to 10-7A and maximum sample magnification of 180000X. Under operation conditions, the material undergoes changes in its structure and composition; there has been a depletion of the constituent elements of the alloy produced by oxidation and carburization. This phenomenon leads to the degradation of the alloy by the formation of a powder consisting of fine particles of metal and carbon. Fig. 1 shows a SEM micrograph where the deposit of graphite on the metal surface is observed, a “toothed” structure of the metal surface by the penetration of the graphite or coke is evident. From the service-exposed material SEM analysis, it was also observed intragranular carbides. Carbides become visible in the grain edge generating internal tension due their big size. The existence of porosities and cracks contribute to reduce the effort propagation towards the substrate, since they act as points of nucleation and crack propagation.

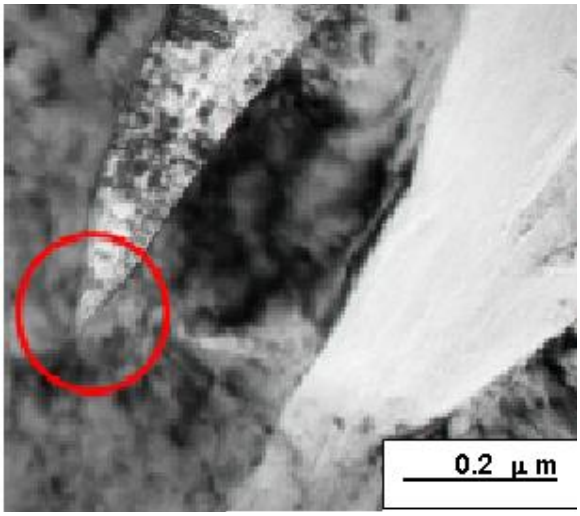

Fig 1: SEM micrograph of the ex-service Fe-25Cr-20Ni-0.40C alloy.

The specimens were also analyzed by optical microscopy [6, 7]. Metallographic examination was carried using an optical microscope (mark: LEICA), with analyzer of images QWIN. It is observed the as-cast alloy microstructure corresponding to an austenitic matrix where long carbides are located in dendritic edges and in the grain edges; while in the service-exposed alloy, it is observed in the austenitic matrix, a great coalescence of carbides of bigger size (Fig. 2).

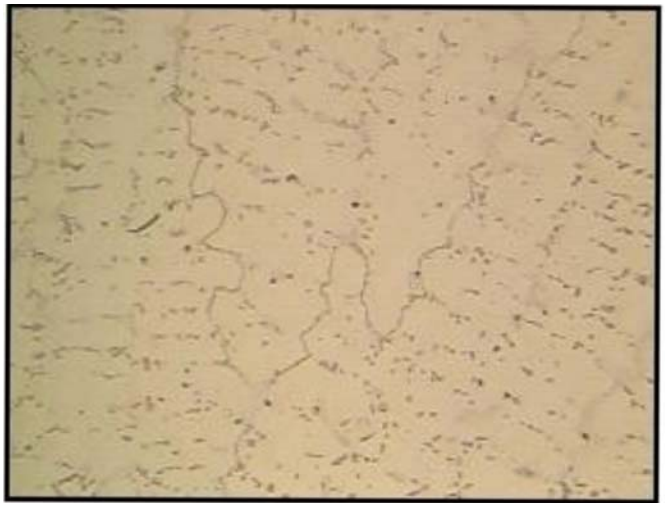

Fig 2: Optical micrographs of the ex-service Fe-25Cr-20Ni-0.40C alloy (400x).

High-temperature corrosion produces a material degradation process that occurs at the surface of the engineering component. In the case of internal corrosion, the corrosive species penetrated into the material by solid-state diffusion leading to the formation of internal precipitates, for instance, carbides. Internal corrosion results in a strong deterioration of the properties of a material. The mechanisms and kinetics of the internal corrosion processes are determined by the temperature, the local chemical composition of the material, the solubility and diffusivity of the corrosive species, as well as the mechanical loading conditions.

3. Computational Study

A theoretical study was performed to analyze the changes in the electronic structure and the chemical bonding after carburization phenomena. The calculations were performed using the Vienna ab initio simulation package VASP [8, 11] which is a DFT code, working in a plane-wave basis set. The electron–ion interaction was described using the projector-augmented-wave (PAW) method with plane waves up to an energy of Ecut = 450 eV. For exchange and correlation the functional proposed by Perdew and Zunger is used, adding (semi-local) generalized gradient corrections (GGA). In order to simulate the Fe-25Cr-20Ni-0.40C alloy, the substrate is modeled by five layers of metal having γ-FeNiCr structure. The three uppermost substrate layers and the carbon impurity are allowed to relax. It was compared the alloy structure before and after the carburization process. The carbon impurity locates near a Ni, Fe and Cr atoms at distances of 1.3 Å, 1.4 Å and 1.7 Å, respectively. As consequence, a Ni-C, Fe-C and Cr-C interactions are formed. The COOP curves for the C-Ni, C-Fe and C-Cr interactions were plotted with the Yet another Extended Huckel Molecular Orbital Package (YAeHMOP) [12] (Fig. 3). The C-metals are mainly bonding interactions and the biggest C-metal overlap population (OP) corresponds to the Ni-C interaction (Ni-C > Fe-C > Cr-C). The atomic orbital occupations of the metallic atoms nearest neighbor to carbon atoms are modified after carburization process. The Ni 4s population decreases to about 13% when the C is present. The Ni 4p populations decrease 2% while the Ni 3d population diminishes to about 1%. This indicates a majority participation of Ni 4s orbital in the Ni-C bonding. On the other hand, the Fe 4s population decreases to about 13% and the Fe 4p populations decrease to about 30%, when the C is present. The Fe 3d population decreases to about 8%. This denoted a greater participation of Fe 4p orbital in the Fe-C bonding. In the case of the Cr atom nearest neighbor to C, the Cr 4s population decreases to about 7% and the contribution of Cr 4p populations decreases 21%; while the Cr 3d population diminishes to about 3%. As predicted by the electronegativity differences, the population analysis brings a partial negative charge on the carbon atoms while positive charge on the close neighbor Ni, Fe and Cr atoms, indicating an electron transfer to the impurity atoms from the metallic nearest neighbors. We observed the most important electron transfer corresponding to Fe nearest neighbor atoms.

The metallic bonds strength is modified after carburization. The Fe-Ni, Cr-Ni, Ni-Ni and Fe-Cr bonds nearest neighbors to carbon atoms are the most affected; their OP diminish to about 80%, 75%, 70% and 60% respectively. The nearest neighbor Fe-Fe and Cr-Cr bonds strength decreases 7% and less to 1%, respectively.

4. Conclusions

This investigation combines microstructural characterization analyses and atomistic modeling to better elucidate the mechanism of carburization embrittlement of iron-nickel-chromium alloys exposed to high temperature.

It was compared two samples of Fe-25Cr-20Ni-0.40C steel, the as-cast material with the same one obtained of the tubes of an industrial cracking furnace after 25,000 h of service at 900-1200 ºC. In the service-exposed material, it was observed bigger carbides in the austenitic matrix comparing with the as-cast material, cavities oriented between grains and

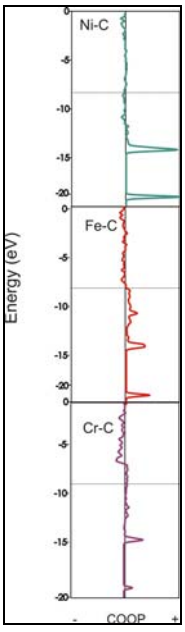

Fig 3 COOP curves for Ni-C, Fe-C and Cr-C interactions.

Some microfissures are observed in grain edges, indicating that the material present damage by creep.

The theoretical calculations help us to interpret the changes observed experimentally by studying the alloy electronic structure and the chemical bonding after the carburization phenomena. The atomic orbital occupations of the metallic

bonds close to the carbon atoms are affected. The mainly changes are presented in Ni 4s, Fe 4p and Cr 4p orbitals. An electron transfer to the carbon atoms from the Ni, Fe and Cr nearest neighbor atoms is observed. The strengths of the Fe-Ni, Cr-Ni, Ni-Ni and Fe-Cr bonds nearest neighbors to carbon atoms are the most affected. The metallic bond weakening is mainly a consequence of the new C-Ni, C-Fe and C-Cr interactions formed after carburization process.

5. Acknowledgments

Our work was supported by SCyT UTN and UNS, PIP-CONICET . A Juan, G Brizuela and S Simonetti are members of CONICET.

6. References

1. ASTM Standards, Annual Book, Metallograpy Nondestructive Testing, Philadelphia;1984, 03.03
2. Russ JC. Uses of the Electron Microscope in the Materials Science, ASTM, STP 480, Philadelphia, 1970, 214.
3. Lee R L, Kelly JF, Pract. Metallogr, 1984; 21:7.
4. Harle JW, The Use of the Scanning Electron Microscope, Pergamon Press; 1972.
5. Mc Gannon H. The Making and Treating of Steel, ASTM, 9 Ed. United Steel, 1220; 1971.
6. Louthan M. Optical Metallography, Departament of Materials, U Virginia Polytechnics Institute, 1985.
7. Beeston B. Electron Doffraction and optical diffraction techniques, North Holland Publishing Co, 1972.
8. Kresse G, Hafner J. Phys. Rev. B, 1993; 47:58.
9. Kresse G, Hafner J. Phys. Rev. B, 1993; 8:3115.
10. Kresse G, Hafner J. Phys. Rev. B, 1994; 49:4251.
11. http://www.vasp.at/
12. Landrum G, Glassey W. Yet Another Extended HuckelMolecular Orbital Package (YAeHMOP) Cornell University, Ithaca, NY 2004.